Preprints of the 21st IFAC World Congress (Virtual)
Berlin, Germany, July 12-17, 2020

Modeling DC-DC converters from measurements of their Harmonic Transfer Function ⋆

Sanda Lefteriu *

* *IMT Lille Douai, Univ. Lille, Unité de Recherche Informatique Automatique, F-59000 Lille, France (e-mail: sanda.lefteriu@imt-lille-douai.fr)*

Abstract: Power converters rely on semiconductor devices (transistors and/or diodes) acting as switches opening and closing periodically, hence they can be analyzed as periodic switched linear systems. The periodic behavior makes it possible to model them via the Harmonic Transfer Function (HTF). The HTF contains an infinite number of transfer functions, relating to each harmonic, but for converters operating in continuous current mode, a limited number of harmonics yields satisfactory results. This extended abstract aims at recovering a state-space model in a system identification sense from frequency-domain measurements that are physically realizable. After analyzing the open-loop response to a range of small-signal inputs with the FFT, the measurements of the HTF are obtained. This data set is used in the Loewner framework to create a descriptor-form continuous model. The advantage of the Loewner framework is that the quantities involved can be expressed in terms of generalized controllability and observability matrices. Hence, the similarity transformation is the extended observability matrix, and an optimization problem can be set up and solved iteratively for recovering the Fourier coefficients of the converter's state-space matrices and, consequently, the full description of the periodic system.

Keywords: Model approximation, Data-driven modeling, Frequency domain identification, Hybrid and switched systems modeling, Periodic systems, Modeling and simulation of power systems.

1. INTRODUCTION

Power converters are electronic circuits allowing the electric power source (a battery, the electrical network, a solar panel, etc.) to be adapted to the needs of the receiver (an electric motor, an asynchronous machine, etc.). Converters can be classified as: DC to DC, DC to AC, AC to DC and AC to AC converters based on the type of current accepted by the supply and the load. This contribution focuses on DC-DC converters, found in mobile phones, laptops, wind turbines, photovoltaic systems, electric cars, etc. Many topologies exist, the easiest to analyze being the buck converter (a step-down converter) and the boost converter (a step-up converter). Fig. 1 shows the circuit diagram of an open-loop buck converter: the transistors and diodes acting as switches make it a switched system. In continuous current mode (CCM), the transistor S is open and closed with a certain switching frequency, while the diode $\overline{S}$ follows the opposite behavior (Fig. 2). Fig. 3 shows the voltage drop over the transistor when assuming ideal switching (in reality, switching is not an instantaneous process). The periodic behavior of the switches dictates the periodicity of the overall system. The output filter is an RLC circuit, hence linear. Thus, DC-DC converters are periodic switched linear (PSL) systems.

This contribution focuses on modeling the buck converter in the frequency domain from physically realizable measurements. Using the small signal paradigm, an AC voltage of small amplitude and varying frequency is added to the DC input. An FFT analysis of the output reveals, besides the perturbation

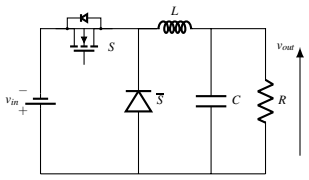

Fig. 1. Circuit diagram for the buck converter

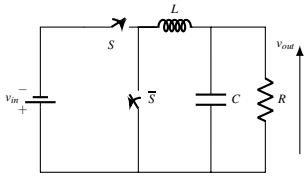

Fig. 2. The buck converter as a switched system

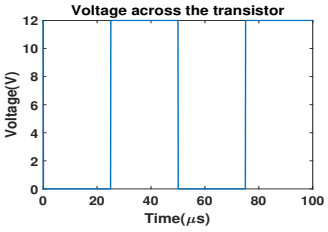

Fig. 3. Ideal switching

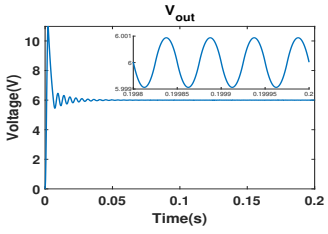

Fig. 4. Converter's response

frequency, other frequencies (typically referred to as harmonic distortions Erickson (1983)). These frequencies are predicted by the Harmonic Transfer Function (HTF), developed as a tool for analyzing periodic systems in the frequency domain. The HTF is expressed in terms of doubly-infinite state-space matrices in terms of the Fourier coefficients of the periodic state-space representation which, for our application, can be truncated to only a few terms. From the spectral analysis of the response to a range of sinusoid perturbations, data at the expected frequencies are gathered, which represent measurements of the HTFs. These can be employed in the Loewner framework, proposed by Mayo and Antoulas (2007), to identify the continuous-form of these HTFs in terms of

⋆ This work has been achieved within the framework of the CE2I project (Convertisseur d'Energie Intégré Intelligent). CE2I is co-financed by European Union with the financial support of European Regional Development Fund (ERDF), the French State and the French Region of Hauts-de-France.

a descriptor-form realization. The advantage of the Loewner framework is that the quantities involved can be expressed in terms of generalized controllability and observability matrices. Hence, the similarity transformation is, in fact, the extended observability matrix and an optimization problem can be set up and solved iteratively for recovering the Fourier coefficients of the converter's state-space matrices and, consequently, the full description of the periodic system.

Typically, the buck converter is characterized by the average model, developed by Middlebrook and Cuk (1976). This is a linear time-invariant model which describes the dynamics of the system in terms of average values for current and voltage variables, neglecting the effects due to switching. This model is valid until half of the switching frequency, when aliasing occurs. High frequency harmonics are, therefore, not captured by the average model. Fig. 4 shows the response of the buck converter to a DC input, a shape similar to the response of a second-order system and what the average model predicts. However, when zooming in, an oscillation with the same frequency as the switching frequency can be detected, which the average model is not able to capture.

Developed for identifying a descriptor representation of LTI systems (Mayo and Antoulas (2007); Lefteriu and Antoulas (2010)) from measurements of their transfer function, Gosea et al. (2018) extended the Loewner framework to the class of linear switched systems. In particular, data used by Gosea et al. (2018) are samples of input-output mappings in the form of a series of multivariate rational functions obtained by taking the multivariate Laplace transform, which cannot be measured physically. The present paper uses the Loewner framework to model the periodic behavior of power converters from data that can be measured easily.

2. MODELING PERIODIC SYSTEMS IN THE FREQUENCY DOMAIN

The converter's dynamics can be written in state-space form as:

$$\dot{\mathbf{x}}(t) = \mathbf{A}(t)\mathbf{x}(t) + \mathbf{b}(t)v_{in}(t) \tag{1}$$
$$v_{out}(t) = \mathbf{c}(t)\mathbf{x}(t) + d(t)v_{in}(t) \tag{2}$$

where $\mathbf{A}(t) \in \mathbb{R}^{n\times n}$, $\mathbf{b}(t) \in \mathbb{R}^{n\times 1}$, $\mathbf{c}(t) \in \mathbb{R}^{1\times n}$, $d(t) \in \mathbb{R}$ are periodic, with period $T_s > 0$, called the switching period: $\mathbf{A}(t) = \mathbf{A}(t+mT_s)$, $\forall m \in \mathbb{Z}$, and the same for $\mathbf{b}(t)$, $\mathbf{c}(t)$, $d(t)$.

For linear time periodic (LTP) systems, a sinusoid input with excitation frequency f_i produces an infinite sum of sinusoid signals at frequencies equal to $f_i + mf_s$, with harmonics of the switching frequency $f_s = \frac{1}{T_s}$, $\forall m \in \mathbb{Z}$. This can be visualized in Fig. 5 from the FFT analysis of the converter's response to a DC superimposed to an AC input with frequency $f_i = 5$kHz. The converter is operating with switching frequency $f_s = 20$kHz.

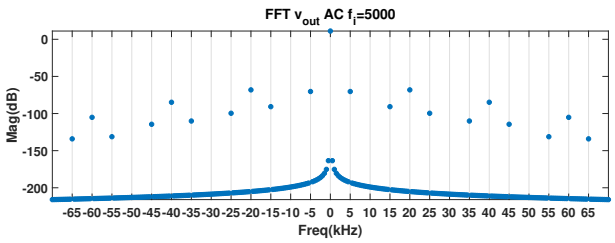

Fig. 5. FFT analysis of response to sum of DC and 5kHz AC inputs (11)

To account for the harmonics induced by the periodic behavior, the concept of Harmonic Transfer Functions (HTFs) was developed by Wereley (1991), with different transfer functions accounting for each harmonic.

Periodic switched systems change between different discrete modes. In continuous conduction mode (CCM), the converter's behavior follows two such modes:

(1) 1^{st} mode: in time interval $t \in [mT_s, (m+D)T_s)$, $\forall m \in \mathbb{Z}$, where $D < 1$ is the duty cycle (the percentage of T_s that the switch is ON). The system dynamics can be expressed using state-space matrices $\mathbf{A}^{(1)}$, $\mathbf{b}^{(1)}$, $\mathbf{c}^{(1)}$, $d^{(1)}$.
(2) 2^{nd} mode: for $t \in [(m+D)T_s, (m+1)T_s)$: switch OFF, with state-space matrices $\mathbf{A}^{(2)}$, $\mathbf{b}^{(2)}$, $\mathbf{c}^{(2)}$, $d^{(2)}$.

This yields the following expression for $\mathbf{A}(t)$, and similarly for $\mathbf{b}(t)$, $\mathbf{c}(t)$ and $d(t)$:

$$\mathbf{A}(t) = \begin{cases} \mathbf{A}^{(1)}, & t \in [mT_s, (m+D)T_s) \\ \mathbf{A}^{(2)}, & t \in [(m+D)T_s, (m+1)T_s) \end{cases}, \forall m \in \mathbb{Z}. \tag{3}$$

As for any periodic signal with period $T_s = \frac{1}{f_s}$, we can express $\mathbf{A}(t)$ in terms of its Fourier Series

$$\mathbf{A}(t) = \sum_{j=-\infty}^{\infty} \mathbf{A}_j \exp^{\mathrm{i}j\omega_s t}, \quad \omega_s = 2\pi f_s, \tag{4}$$

and similarly for $\mathbf{b}(t)$, $\mathbf{c}(t)$ and $d(t)$. The Fourier coefficients $\mathbf{A}_j$ can be computed by the usual formula

$$\mathbf{A}_j = \frac{1}{T_s}\int_0^{T_s} \mathbf{A}(t)\exp^{-\mathrm{i}j\omega_s t}\, dt. \tag{5}$$

Similar expressions are available for the Fourier coefficients of the $\mathbf{b}$, $\mathbf{c}$ and d quantities. Substituting these into (1)-(2), applying the Laplace Transform leads to a compact form:

$$\mathrm{s}\mathcal{X}(\mathrm{s}) = (\mathcal{A} - \mathcal{N})\mathcal{X}(\mathrm{s}) + \mathcal{B}\mathcal{V}_{in}(\mathrm{s}) \tag{6}$$
$$\mathcal{V}_{out}(\mathrm{s}) = \mathcal{C}\mathcal{X}(\mathrm{s}) + \mathcal{D}\mathcal{V}_{in}(\mathrm{s}), \tag{7}$$

by defining doubly-infinite matrices $\mathcal{A}$, $\mathcal{B}$, $\mathcal{C}$ and $\mathcal{D}$ that are Toeplitz matrices and $\mathcal{N}$ that is block diagonal:

$$\mathcal{A} = \begin{bmatrix} \ddots & \vdots & \vdots & \vdots & \iddots \\ \dots & \mathbf{A}_0 & \mathbf{A}_{-1} & \mathbf{A}_{-2} & \dots \\ \dots & \mathbf{A}_1 & \mathbf{A}_0 & \mathbf{A}_{-1} & \dots \\ \dots & \mathbf{A}_2 & \mathbf{A}_1 & \mathbf{A}_0 & \dots \\ \iddots & \vdots & \vdots & \vdots & \ddots \end{bmatrix}, \mathcal{N} = \begin{bmatrix} \ddots & & & & \\ & -\mathrm{i}\omega_s\mathbf{I} & & & \\ & & \mathbf{0} & & \\ & & & \mathrm{i}\omega_s\mathbf{I} & \\ & & & & \ddots \end{bmatrix}, \tag{8}$$

where $\mathcal{X}(\mathrm{s}) = [\dots \mathbf{X}_{-1}(\mathrm{s}+\mathrm{i}\omega_s)\ \mathbf{X}_0(\mathrm{s})\ \mathbf{X}_1(\mathrm{s}-\mathrm{i}\omega_s)\ \dots]^T$, $\mathcal{V}_{in}(\mathrm{s}) = [\dots V_{in_{-1}}(\mathrm{s}+\mathrm{i}\omega_s)\ V_{in_0}(\mathrm{s})\ V_{in_1}(\mathrm{s}-\mathrm{i}\omega_s)\ \dots]^T$ and similarly $\mathcal{V}_{out}(\mathrm{s})$ are infinite vectors, where $\mathbf{X}_j$, V_{in_j}, V_{out_j}, $j = -\infty, \dots, \infty$ are the Fourier coefficients of the corresponding time-domain signals in the ω_s-basis. The Harmonic Transfer Function, relating harmonics of the output to harmonics of the input signal: $\mathcal{V}_{out}(\mathrm{s}) = \mathcal{H}(\mathrm{s})\mathcal{V}_{in}(\mathrm{s})$, is defined as

$$\mathcal{H}(\mathrm{s}) = \mathcal{C}\left(\mathrm{s}\mathbf{I} - (\mathcal{A} - \mathcal{N})\right)^{-1}\mathcal{B} + \mathcal{D} \tag{9}$$

$$= \begin{bmatrix} \ddots & \vdots & \vdots & \vdots & \iddots \\ \dots & \mathrm{H}_0(\mathrm{s}+\mathrm{i}\omega_s) & \mathrm{H}_{-1}(\mathrm{s}) & \mathrm{H}_{-2}(\mathrm{s}-\mathrm{i}\omega_s) & \dots \\ \dots & \mathrm{H}_1(\mathrm{s}+\mathrm{i}\omega_s) & \mathrm{H}_0(\mathrm{s}) & \mathrm{H}_{-1}(\mathrm{s}-\mathrm{i}\omega_s) & \dots \\ \dots & \mathrm{H}_2(\mathrm{s}+\mathrm{i}\omega_s) & \mathrm{H}_1(\mathrm{s}) & \mathrm{H}_0(\mathrm{s}-\mathrm{i}\omega_s) & \dots \\ \iddots & \vdots & \vdots & \vdots & \ddots \end{bmatrix}. \tag{10}$$

For converters operating in CCM, few harmonics (say N) are needed (Love (2007)), so infinite quantities can be truncated to dimension $2N+1$, with the sum ranging from $-N$ to N.

3. COMPUTATIONAL ASPECTS

To ensure correct operation for the DC-DC converter, the input is a constant voltage superimposed to an AC component with amplitude several orders of magnitude smaller ($v_{DCin} \gg v_{ACin}$):

$$v_{in}(t) = v_{DCin} + v_{ACin}\cos(2\pi f_i t), \tag{11}$$

with f_i, the perturbation frequency. Its Laplace transform is $\mathcal{V}_{in}(\mathrm{s}) = [\ \dots\ 0\ V_{in_0}(\mathrm{s})\ 0\ \dots\ ]^T$. The response contains, besides f_i, harmonics at $f_i + mf_s$, $m \in \mathbb{Z}$ (recall Fig. 5):

$$v_{ACout}(t) = \sum_{m=-\infty}^{\infty} v_{ACm}\cos(2\pi(f_i + mf_s)t + \phi_{ACm}). \tag{12}$$

In the Laplace domain, this amounts to expressing

$$\mathcal{V}_{out}(\mathrm{s}) = \begin{bmatrix} \vdots \\ V_{out_{-1}}(\mathrm{s}+\mathrm{i}\omega_s) \\ V_{out_0}(\mathrm{s}) \\ V_{out_1}(\mathrm{s}-\mathrm{i}\omega_s) \\ \vdots \end{bmatrix} = \underbrace{\begin{bmatrix} \vdots \\ \mathrm{H}_{-1}(\mathrm{s}) \\ \mathrm{H}_0(\mathrm{s}) \\ \mathrm{H}_1(\mathrm{s}) \\ \vdots \end{bmatrix}}_{\mathcal{H}(\mathrm{s})} V_{in_0}(\mathrm{s}). \tag{13}$$

Through an FFT analysis of the output, the amplitude and phase of the harmonics are determined and the measurements of the HTF established: $H_m(\mathrm{i}\omega_i) = \frac{v_{ACm}}{v_{ACin}}\exp^{\mathrm{i}\phi_{ACm}}, m = -N, \dots, 0, \dots, N$.

4. THE LOEWNER FRAMEWORK

Given pairs of the form $(f_i, \mathbf{H}_i)$, $i = 1, \dots, P$, where $\mathbf{H}_i \in \mathbb{C}^{q\times p}$ is the MIMO transfer function measured at f_i, we partition the set of points $\{\mathrm{i}\omega_1, -\mathrm{i}\omega_1, \dots, \mathrm{i}\omega_P, -\mathrm{i}\omega_P\} = \{\lambda_1, \dots, \lambda_P\} \cup \{\mu_1, \dots, \mu_P\}$ into right λ_k, $k = 1, \dots, P$ and left points μ_h, $h = 1, \dots, P$. It is advisable to consider odd frequencies f_i as right data and even frequencies as left data. We select right tangential directions as column vectors $\mathbf{r}_k$ and left directions as row vectors $\mathbf{l}_h$, for simplicity, as vectors of the identity matrix, as suggested in Lefteriu and Antoulas (2010). Matrix data $\mathbf{H}_i$ becomes right vector data $\mathbf{H}_k\mathbf{r}_k = \mathbf{w}_k$ and left vector data $\mathbf{l}_h\mathbf{H}_h = \mathbf{v}_h$. Collecting these into $\mathbf{\Lambda} = \mathrm{diag}[\,\lambda_1\ \dots\ \lambda_P\,]$, $\boldsymbol{M} = \mathrm{diag}[\,\mu_1\ \dots\ \mu_P\,]$, $\mathbf{R} = [\,\mathbf{r}_1\ \dots\ \mathbf{r}_P\,]$, $\mathbf{W} = [\,\mathbf{w}_1\ \dots\ \mathbf{w}_P\,]$, $\mathbf{L} = [\,\mathbf{l}_1\ \dots\ \mathbf{l}_P\,]^T$, $\mathbf{V} = [\,\mathbf{v}_1\ \dots\ \mathbf{v}_P\,]^T$ and defining the Loewner and shifted Loewner matrices, entry-wise, as

$$\mathbb{L}_{hk} = \frac{\mathbf{v}_h\mathbf{r}_k - \ell_h\mathbf{w}_k}{\mu_h - \lambda_k}, \sigma\mathbb{L}_{hk} = \frac{\mu_h\mathbf{v}_h\mathbf{r}_k - \lambda_k\ell_h\mathbf{w}_k}{\mu_h - \lambda_k}, h, k = 1, \dots, P, \tag{14}$$

we can write a non-minimal descriptor realization of the transfer function $\mathbf{H}(\mathrm{s}) = \mathbf{W}(\sigma\mathbb{L} - \mathrm{s}\mathbb{L})^{-1}\mathbf{V}$ satisfying the right and left interpolation conditions $\mathbf{H}(\lambda_k)\mathbf{r}_k = \mathbf{w}_k$ and $\mathbf{l}_h\mathbf{H}(\mu_h) = \mathbf{v}_h$ (Mayo and Antoulas (2007)). The Loewner matrix being equivalent to the Hankel matrix for frequency-domain data, similar relationships involving generalized controllability and observability matrices exist: $\mathbb{L} = -O\mathcal{R}$, $\sigma\mathbb{L} = -O\mathbf{A}\mathcal{R}$, while $\mathbf{W} = \mathbf{C}\mathcal{R}$ and $\mathbf{V} = O\mathbf{B}$, where the underlying system generating the data is $\mathbf{H}(\mathrm{s}) = \mathbf{C}(\mathrm{s}\mathbf{I} - \mathbf{A})^{-1}\mathbf{B}$ and, in Matlab notation,

$$O(h,:) = \left[\ell_h\mathbf{C}(\mu_h\mathbf{I} - \mathbf{A})^{-1}\right], \mathcal{R}(:,k) = \left[(\lambda_k\mathbf{I} - \mathbf{A})^{-1}\mathbf{B}\mathbf{r}_k\right]. \tag{15}$$

To obtain a minimal realization, we perform a singular value decomposition $[\mathbf{Y}, \Sigma, \mathbf{X}] = \mathrm{svd}(\sigma\mathbb{L} - x\mathbb{L})$, for some $x \in \{f_i\}$. Choosing n as the singular value where the largest drop occurs, we define $\mathbf{X}_n = \mathbf{X}(:, 1:n)$ and $\mathbf{Y}_n = \mathbf{Y}(:, 1:n)^*$. The model of size n is $\widehat{\mathbb{L}} = -\mathbf{Y}_n\mathbb{L}\mathbf{X}_n$, $\widehat{\sigma\mathbb{L}} = -\mathbf{Y}_n\sigma\mathbb{L}\mathbf{X}_n$, $\widehat{\mathbf{V}} = \mathbf{Y}_n\mathbf{V}$, $\widehat{\mathbf{W}} = \mathbf{W}\mathbf{X}_n$. After some state transformations, the details of which can be found in (Antoulas et al., 2017, Sect. 2.3.1), the truncated matrices can be recast as quantities embedding interpolation conditions at $2n$ new points: $\widetilde{\mathbf{\Lambda}}$, $\widetilde{\mathbf{R}}$, $\widetilde{\mathbf{W}}$, $\widetilde{M}$, $\widetilde{\mathbf{L}}$, $\widetilde{\mathbf{V}}$, $\widetilde{\mathbb{L}}$, $\widetilde{\sigma\mathbb{L}}$.

To recover the truncated matrices from (9), we seek the similarity transformation $\mathbf{T}$ between the unknown realization $(\mathcal{A}_N - \mathcal{N}_N, \mathcal{B}_N, \mathcal{C}_N)$ and the one found with the Loewner framework $\left(\widetilde{\sigma\mathbb{L}}\widetilde{\mathbb{L}}^{-1}, \widetilde{\mathbf{V}}, -\widetilde{\mathbf{W}}\widetilde{\mathbb{L}}^{-1}\right)$:

$$\mathbf{T}\widetilde{\sigma\mathbb{L}}\widetilde{\mathbb{L}}^{-1}\mathbf{T}^{-1} = \mathcal{A}_N - \mathcal{N}_N,\ \mathcal{B}_N = \mathbf{T}\widetilde{\mathbf{V}},\ \mathcal{C}_N = -\widetilde{\mathbf{W}}\widetilde{\mathbb{L}}^{-1}\mathbf{T}^{-1}. \tag{16}$$

This is a grey-box estimation problem and approaches such as Xie and Ljung (2002) can be employed. Note that both $\mathbf{T}$, as well as the Fourier coefficients in $\mathcal{A}_N$, $\mathcal{B}_N$, $\mathcal{C}_N$ are unknowns. However, making use of the relationships involving the generalized controllability and observability matrices for the truncated matrices, we find that

$$\mathbf{T}^{-1} = O = \begin{bmatrix} \widetilde{\ell}_1\mathcal{C}_N(\widetilde{\mu}_1\mathbf{I} - (\mathcal{A}_N - \mathcal{N}_N))^{-1} \\ \vdots \\ \widetilde{\ell}_n\mathcal{C}_N(\widetilde{\mu}_n\mathbf{I} - (\mathcal{A}_N - \mathcal{N}_N))^{-1} \end{bmatrix}. \tag{17}$$

Hence, the unknowns are only the Fourier coefficients $\mathbf{A}_0$, $\mathbf{A}_{\pm1}$, $\mathbf{A}_{\pm2}$ and $\mathbf{c}_0$ in (5) and (8). From initial guesses for the Fourier coefficients, we can form $\mathcal{A}_N$ and $\mathcal{C}_N$ in (17) and, afterwards, rewrite (16) as an optimization problem

$$\begin{aligned}\min \|\widetilde{\sigma\mathbb{L}}\widetilde{\mathbb{L}}^{-1}\mathbf{T}^{-1} - \mathbf{T}^{-1}(\mathcal{A}_N - \mathcal{N}_N)\|_F + \|\mathbf{T}^{-1}\mathcal{B}_N - \widetilde{\mathbf{V}}\|_F + \\ \|\mathcal{C}_N + \widetilde{\mathbf{W}}\widetilde{\mathbb{L}}^{-1}\mathbf{T}^{-1}\|_F.\end{aligned} \tag{18}$$

which can be solved iteratively for $\mathbf{A}_0$, $\mathbf{A}_{\pm1}$, $\mathbf{A}_{\pm2}$, $\mathbf{b}_0$, $\mathbf{b}_{\pm1}$ and $\mathbf{c}$. Note that, to ensure identifiability, the number of unknowns, $2n^2 + 3n$, where n is the order of the system in (1), should be smaller than $n_x(n_u + n_y) = (2N+1)n(2N+2)$, as indicated in Ljung (1999). From these Fourier coefficients, we deduce what the state-space matrices in each discrete mode are.

5. THE BUCK CONVERTER AS A PSL SYSTEM

5.1 Ideal system

This section considers ideal switches, which turn ON or OFF instantaneously. The circuit is modeled by differential equations involving the capacitor's voltage $v_C(t)$ and the inductor's current $i_L(t)$ in each working mode $i = 1, 2$:

$$\dot{\mathbf{x}}(t) = \mathbf{A}\mathbf{x}(t) + \mathbf{b}^{(i)}v_{in}(t),\ \mathbf{x}(t) = \begin{bmatrix} V_C(t) \\ I_L(t) \end{bmatrix}, \tag{19}$$

$$\mathbf{A} = \begin{bmatrix} -\frac{1}{RC} & \frac{1}{C} \\ -\frac{1}{L} & 0 \end{bmatrix},\ \mathbf{b}^{(1)} = \begin{bmatrix} 0 \\ \frac{1}{L} \end{bmatrix},\ \mathbf{b}^{(2)} = \begin{bmatrix} 0 \\ 0 \end{bmatrix}. \tag{20}$$

The response is $v_{out}(t) = v_C(t)$, yielding $\mathbf{c} = [1\ 0]$ and $d = 0$ for the output equation $v_{out}(t) = \mathbf{c}\mathbf{x}(t) + dv_{in}(t)$. In this case, $\mathbf{A}$, $\mathbf{c}$ and d are the same for both modes. This allows to simplify the matrices appearing in the HTF: $\mathcal{A} = \mathrm{blkdiag}[\dots, \mathbf{A}, \mathbf{A}, \mathbf{A}, \dots]$, $\mathcal{C} = \mathrm{blkdiag}[\dots, \mathbf{c}, \mathbf{c}, \mathbf{c}, \dots]$, $\mathcal{D} = \mathbf{0}$, while $\mathcal{B}$ is full with Fourier coefficients. Hence, the different HTFs can be decoupled: $\mathrm{H}_j(\mathrm{s}) = \mathbf{c}(\mathbf{I} - (\mathbf{A} - \mathrm{ij}\omega_s\mathbf{I}))^{-1}\mathbf{b}_j$. The average model is precisely the HTF $H_0(\mathrm{s}) = \mathbf{c}(\mathrm{s}\mathbf{I} - \mathbf{A})^{-1}\mathbf{b}_0$, as $\mathbf{b}_0 = D\mathbf{b}^{(1)} + (1-D)\mathbf{b}^{(2)}$.

5.2 Considering the parasitic ON resistance of semiconductors

In reality, the transistor and diode do not switch instantaneously. In this section, the parasitic resistance r_{ton} and r_{don} in series with the corresponding ideal switch is accounted for, yielding different $\mathbf{A}$ matrices for each discrete mode:

$$\mathbf{A}^{(1)} = \begin{bmatrix} -\frac{1}{RC} & \frac{1}{C} \\ -\frac{1}{L} & -\frac{r_{ton}}{L} \end{bmatrix} \text{ and } \mathbf{A}^{(2)} = \begin{bmatrix} -\frac{1}{RC} & \frac{1}{C} \\ -\frac{1}{L} & -\frac{r_{don}}{L} \end{bmatrix}. \tag{21}$$

The rest of the matrices are as in Sect. 5.1. The doubly-infinite matrix $\mathcal{A}$ in (8) is full with Fourier coefficients and the HTFs can no longer be decoupled. The harmonic transfer functions should be modeled together as a SIMO system.

5.3 Numerical example

A Matlab 2019a Simulink model (Srinivasan (2019)) of a buck converter with $L = 1\text{mH}$, $C = 500\mu\text{F}$, $R = 12\Omega$, $f_s = 20\text{kHz}$, $v_{DCin} = 12V$ and duty cycle $D = \frac{1}{2}$ was considered. The chosen values for R_{on} are $R_{ton} = .2$ and $R_{don} = .01$ for the transistor and the diode. Due to space limitations, only the case accounting for parasitics is discussed, the ideal system being easier to analyse. The infinite matrices in $\mathcal{H}(\text{s})$ are truncated to $N = 1$:

$$\mathcal{A}_N = \begin{bmatrix} \mathbf{A}_0 & \mathbf{A}_{-1} & \mathbf{A}_{-2} \\ \mathbf{A}_1 & \mathbf{A}_0 & \mathbf{A}_{-1} \\ \mathbf{A}_2 & \mathbf{A}_1 & \mathbf{A}_0 \end{bmatrix}, \ \mathcal{B}_N = \begin{bmatrix} \mathbf{b}_{-1} \\ \mathbf{b}_0 \\ \mathbf{b}_1 \end{bmatrix}, \ \mathcal{C}_N = \begin{bmatrix} \mathbf{c} & & \\ & \mathbf{c} & \\ & & \mathbf{c} \end{bmatrix}. \quad (22)$$

The Fourier coefficients have the following numerical values:

$$\mathbf{A}_0 = \begin{bmatrix} -166.67 & 2000 \\ -1000 & 105 \end{bmatrix}, \mathbf{A}_{\pm 1} = \mp \frac{\text{i}}{\pi} \begin{bmatrix} 0 & 0 \\ 0 & -190 \end{bmatrix}, \mathbf{A}_{\pm 2} = \mathbf{0}, \quad (23)$$

$$\mathbf{b}_0 = \begin{bmatrix} 0 \\ 500 \end{bmatrix}, \mathbf{b}_{\pm 1} = \mp \frac{\text{i}}{\pi} \begin{bmatrix} 0 \\ 1000 \end{bmatrix}, \ \mathbf{c} = [\,1 \ 0\,]. \quad (24)$$

Responses $V_{out_{-1}}(\text{i}\omega_i + \text{i}\omega_s)$, $V_{out_0}(\text{i}\omega_i)$ and $V_{out_1}(\text{i}\omega_i - \text{i}\omega_s)$ to perturbation frequencies $f_i = 10,15,20,\ldots,100,150,200,\ldots,1\text{k}$, $1.5\text{k},2\text{k},\ldots,19\text{k},19050,19100,\ldots,19900,19905,\ldots,19995\text{Hz}$, in total 108 points, were used in the FFT analysis, yielding $H_{-1}(s)$, $H_0(s)$ and $H_1(s)$ as HTFs to be identified as in (13). The Loewner framework identifies the SIMO HTFs from the matrix measurement $\mathbf{H}_i$ of size 3×1. We expect a system of order 6, due to the matrix $\mathcal{A}_N - \mathcal{N}_N$ having size 6. Appending the complex conjugate information $H_{-1}(-\text{i}\omega_j) = \overline{H_1(\text{i}\omega_j)}$, $H_0(-\text{i}\omega_j) = \overline{H_0(\text{i}\omega_j)}$, $H_1(-\text{i}\omega_j) = \overline{H_{-1}(\text{i}\omega_j)}$, we identify an order 6 system, as expected: Fig. 6 shows a drop of several orders of magnitude after the 6^{th} singular value of the Loewner and shifted Loewner matrices and Fig. 7 shows that the 6 poles are recovered, the difference in the real parts being negligible.

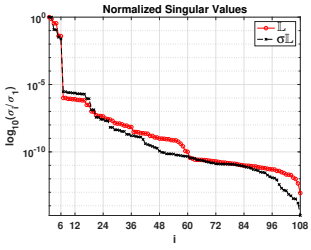

Fig. 6. SVD of the Loewner matrix pencil

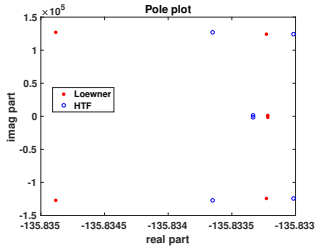

Fig. 7. Poles of the order 6 systems

Fig. 8, 9 and 10 show the magnitude of $H_{-1}(s)$, $H_0(s)$ and $H_1(s)$ evaluated for positive frequencies: the recovered models match the data, as well as the theoretical HTFs. The effect of the ON resistances can be seen in $H_1(s)$, namely the dip around 200Hz.

For some initial guess in the neighborhood of the values given in (23)-(24), using Matlab's `fminunc` function, we can solve the optimization problem in (18) and find better estimates.

6. CONCLUSION AND FUTURE WORK

This extended abstract presents a first step towards modeling DC-DC power converters as periodic switched linear systems

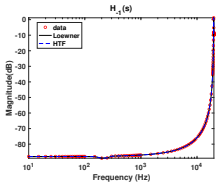

Fig. 8. $H_{-1}(\text{s})$

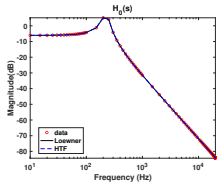

Fig. 9. $H_0(\text{s})$

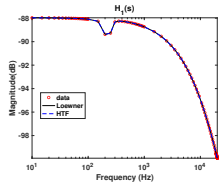

Fig. 10. $H_1(\text{s})$

and their approximation from frequency domain measurements which are physically achievable. The theory presented relies on the identification of harmonic transfer functions in the Loewner framework. When converters operate in closed-loop, the switching signal is obtained through Pulse Width Modulation and the control signal can be considered as an extra input (Yue et al. (2019)). Future work will also account for the control-to-output transfer function in the modeling procedure by considering a similar analysis through the HTF.

REFERENCES

Antoulas, A.C., Lefteriu, S., and Ionita, A.C. (2017). *Model Reduction and Approximation*, chapter 8, 335–376.

Erickson, R.W. (1983). *Large signals in switching converters*. Ph.D. thesis, California Institute of Technology.

Gosea, I.V., Petreczky, M., and Antoulas, A.C. (2018). Data-driven model order reduction of linear switched systems in the Loewner framework. *SIAM Journal on Scientific Computing*, 40(2), B572–B610.

Lefteriu, S. and Antoulas, A.C. (2010). A new approach to modeling multiport systems from frequency-domain data. *IEEE Transactions on Computer-Aided Design of Integrated Circuits and Systems*, 29(1), 14–27.

Ljung, L. (1999). *System Identification (2nd Ed.): Theory for the User*. Prentice Hall PTR, USA.

Love, G.N. (2007). *Small signal modeling of power electronic converters, for the study of time-domain waveforms, harmonic domain spectra, and control interactions*. Ph.D. thesis, University of Canterbury.

Mayo, A. and Antoulas, A. (2007). A framework for the solution of the generalized realization problem. *Linear Algebra and its Applications*, 425(2), 634 – 662.

Middlebrook, R.D. and Cuk, S. (1976). A general unified approach to modeling switching-converter power stages. In *IEEE Power Electronics Specialists Conference*, 18–34.

Srinivasan, K. (2019). Buck-converter open loop, MATLAB Central File Exchange. URL `https://www.mathworks.com/matlabcentral/fileexchange/69285-buck-converter-open-loop`.

Wereley, N. (1991). *Analysis and Control of Linear Periodically Time Varying Systems*. Ph.D. thesis, Massachusetts Institute of Technology.

Xie, L.L. and Ljung, L. (2002). Estimate physical parameters by black-box modeling. *Proceedings of the 21st Chinese Control Conference*.

Yue, X., Wang, X., and Blaabjerg, F. (2019). Review of small-signal modeling methods including frequency-coupling dynamics of power converters. *IEEE Transactions on Power Electronics*, 34(4), 3313–3328.